AMERICAN SOCIETY FOR MICROBIOLOGY | Journal of Clinical Microbiology®

VIROLOGY

Development of Novel PCR Assays for Improved Detection of Enterovirus D68

Tatsuki Ikuse,[a] Yuta Aizawa,[a] Hayato Takihara,[b] Shujiro Okuda,[b,c] Kanako Watanabe,[d] Akihiko Saitoh[a]

[a]Department of Pediatrics, Niigata University Graduate School of Medical and Dental Sciences, Niigata, Japan
[b]Division of Bioinformatics, Niigata University Graduate School of Medical and Dental Sciences, Niigata, Japan
[c]Medical AI Center, Niigata University School of Medicine, Niigata, Japan
[d]Department of Laboratory Science, Niigata University Graduate School of Health Sciences, Niigata, Japan

ABSTRACT Enterovirus D68 (EV-D68) causes a range of clinical manifestations, including asthma-like illness, severe respiratory disease, and acute flaccid myelitis. EV-D68 has caused worldwide outbreaks since 2014 and is now recognized as a reemerging infection in many countries. EV-D68-specific PCR assays are widely used for the diagnosis of EV-D68 infection; however, assay sensitivity is a concern because of genetic changes in recently circulated EV-D68. To address this, we summarized EV-D68 sequences from previously reported world outbreaks from 2014 through 2020 on GenBank, and found several mutations at the primer and probe binding sites of the existing EV-D68-specific PCR assays. Subsequently, we designed two novel assays corresponding to the recently reported EV-D68 sequences: an EV-D68-specific real-time and seminested PCR. In an analysis of 22 EV-D68 confirmed cases during a recent EV-D68 outbreak in Japan, the new real-time PCR had higher sensitivity than the existing assay (100% versus 45%, $P < 0.01$) and a lower median C_T value (27.8 versus 32.8, $P = 0.005$). Sensitivity was higher for the new nonnested PCR (91%) than for the existing seminested PCR assay (50%, $P < 0.01$). The specificity of the new real-time PCR was 100% using samples from non-EV-D68-infected cases ($n = 135$). In conclusion, our novel assays had higher sensitivity than the existing assay and might lead to more accurate diagnosis of recently circulating EV-D68. To prepare for future EV-D68 outbreaks, EV-D68-specific assays must be continuously monitored and updated.

KEYWORDS acute flaccid paralysis, enterovirus D68, real-time PCR, transverse myelitis, *in silico*

Enterovirus D68 (EV-D68) infection causes a range of clinical manifestations, including asthma-like illness, severe respiratory disease, and acute flaccid myelitis (AFM) (1). It was first isolated in 1962 from children with lower respiratory infections in the United States (2). Until 2014, EV-D68 had been detected sporadically (3). However, after a large outbreak in the United States in 2014 and successive outbreaks worldwide almost every 2 years since 2014, EV-D68 is now regarded as a reemerging infection in many countries (4, 5). It is currently included in national surveillance for respiratory infections in the United States and European countries because of its potential for periodic outbreaks (6, 7).

To diagnose EV infection, real-time PCR assays targeting the 5′ noncoding region of EV have been used to detect all EV types. In addition, assays targeting the viral protein 1 (VP1) region have been used for rapid screening of defined EV types (e.g., EV-A71 and EV-D68) for surveillance (8–10). After detection of EV, VP1 sequencing is the gold standard for EV typing (9). EV-D68 has four major clades (A to D) (4, 5), and recent worldwide EV-D68 outbreaks have distinctive clade characteristics. Clade B3 is currently dominant worldwide (5). The dominant clade was recently identified by VP1

Citation Ikuse T, Aizawa Y, Takihara H, Okuda S, Watanabe K, Saitoh A. 2021. Development of novel PCR assays for improved detection of enterovirus D68. J Clin Microbiol 59:e01151-21. https://doi.org/10.1128/JCM.01151-21.

Editor Michael J. Loeffelholz, Cepheid

Address correspondence to Akihiko Saitoh, asaitoh@med.niigata-u.ac.jp.

Received 16 May 2021
Returned for modification 1 June 2021
Accepted 17 August 2021
Accepted manuscript posted online 25 August 2021
Published 19 October 2021

sequencing performed after detection by EV-D68-specific or -nonspecific real-time PCR (5, 11–14).

EV-D68-specific real-time PCR assays used in recent studies were mainly designed by using sequences obtained from worldwide outbreaks in 2014 (10, 15). Notably, a real-time PCR assay initially designed by Washington University (WashU assay) in 2015 (10) has been widely used to detect EV-D68. This assay was reported to be superior to an assay developed in 2014 by the U.S. Centers for Disease Control and Prevention (CDC), which had lower sensitivity, and to commercially available assays (10). However, we recently observed a low success rate for the WashU assay in detecting EV-D68 in samples from a 2018 EV-D68 outbreak in Japan (5). Although WashU yielded negative results for EV-D68 in more than half the samples, subsequent electrophoresis for PCR products confirmed the targeting bands of all samples, indicating successful amplification without proper attachment of the probe (5). In addition, based on our limited sample analysis, EV-D68 testing for the same samples by both VP1 sequence analysis using seminested PCR with the consensus degenerate hybrid oligonucleotide primer (CODEHOP) approach (16), and another PCR assay suggested by the CDC (5) yielded unsatisfactory positive rates of 14% (3/22) and 50% (11/22), respectively.

EV-D68 is usually detected by EV-D68-specific real-time PCR and/or EV typing with VP1 sequencing by seminested PCR after EV real-time PCR. Our recent experience suggested that recent EV-D68 infections might be underdiagnosed because recent genetic changes in circulating EV-D68 in the world have caused a sequence mismatch that decreases the sensitivity of existing assays.

The objectives of this study were to determine why detection rates for the currently used EV-D68 assay are unsatisfactory and to develop improved assays that can detect recent EV-D68 strains.

MATERIALS AND METHODS

Samples. To analyze the assays, we selected samples from three patient groups.

(i) Samples from EV-D68-infected patients. We selected 22 EV-D68-positive nasopharyngeal samples from children younger than age 15 years with asthma-like respiratory illness during the EV-D68 outbreak in Niigata, Japan, in 2018 (5). EV-D68 was detected by either the EV real-time PCR assay (17) or the WashU assay (10). EV-D68 diagnosis was confirmed by genetic sequencing of the VP1 region by either the CDC assays (5) or an additional PCR assay (see Table S1 in the supplemental material).

(ii) Samples from non-EV-D68-infected patients. We selected 135 samples collected during the period from 2014 through 2019 from children younger than age 15 years with aseptic meningitis, acute encephalopathy/encephalitis, or severe respiratory infection. PCR confirmed a non-EV-D68-related diagnosis. The samples were stored in our laboratory, as described in Table S2A in the supplemental material.

(iii) Samples from patients with acute flaccid paralysis. We selected 32 samples from 11 patients with acute flaccid paralysis (AFP) in 2015 or 2018 during the EV-D68 outbreaks in Japan. The samples were collected to identify the pathogens upon admission. The details of the samples collected from the patients are shown in Table S2B. In our previous testing of the 32 samples, 1 sample from 2015 was positive with EV real-time PCR (17), and EV-D68 was confirmed by VP1 sequencing using the CODEHOP approach (16).

RNA extraction. All samples stored in our laboratory were extracted for viral RNA with a QIAamp MinElute virus spin kit (Qiagen, Valencia, CA) (18).

Evaluation of previous EV-D68-specific PCR assays. To optimize the WashU assay and CODEHOP approach for recent EV-D68 strains, we quoted and summarized EV-D68 sequences from previously reported world outbreaks from 2014 through 2020 on GenBank (https://www.ncbi.nlm.nih.gov/genbank/) and identified the binding sites of each primer and probe on the sequences (Table 1; see also Tables S3 to S7) (4, 5, 10, 11, 16, 19–24).

Designs of new assays. First, we designed the novel enterovirus D68-specific real-time PCR assay (NU assay) and novel primer set (N-Set) for the second PCR of seminested PCR (Table 2). To design the assays, we identified and compared binding sites of each primer and probe of WashU (10) and CODEHOP (16) in previously reported EV-D68 sequences (Table 1; see also Tables S3 to S7), which were the strains that caused global outbreaks between 2014 and 2020. A total of 81 sequences of EV-D68 circulated in the United States, Europe, and Asia were obtained from GenBank. We identified variations of each binding site of the primer and probe using the A Plasmid Editor (ApE) version 2.0.59 (https://jorgensen.biology.utah.edu/wayned/ape/) and designed primers and probes to optimize for the variations described in Fig. S2.

EV-D68 PCR assays. Because of the low EV-D68 detection rates for patients with clinically suspected EV-D68 infection during the outbreak, we created two novel assays that corresponded to recent genetic

TABLE 1 Genetic changes in the primer and probe binding sites of the Washington University (WashU) assay

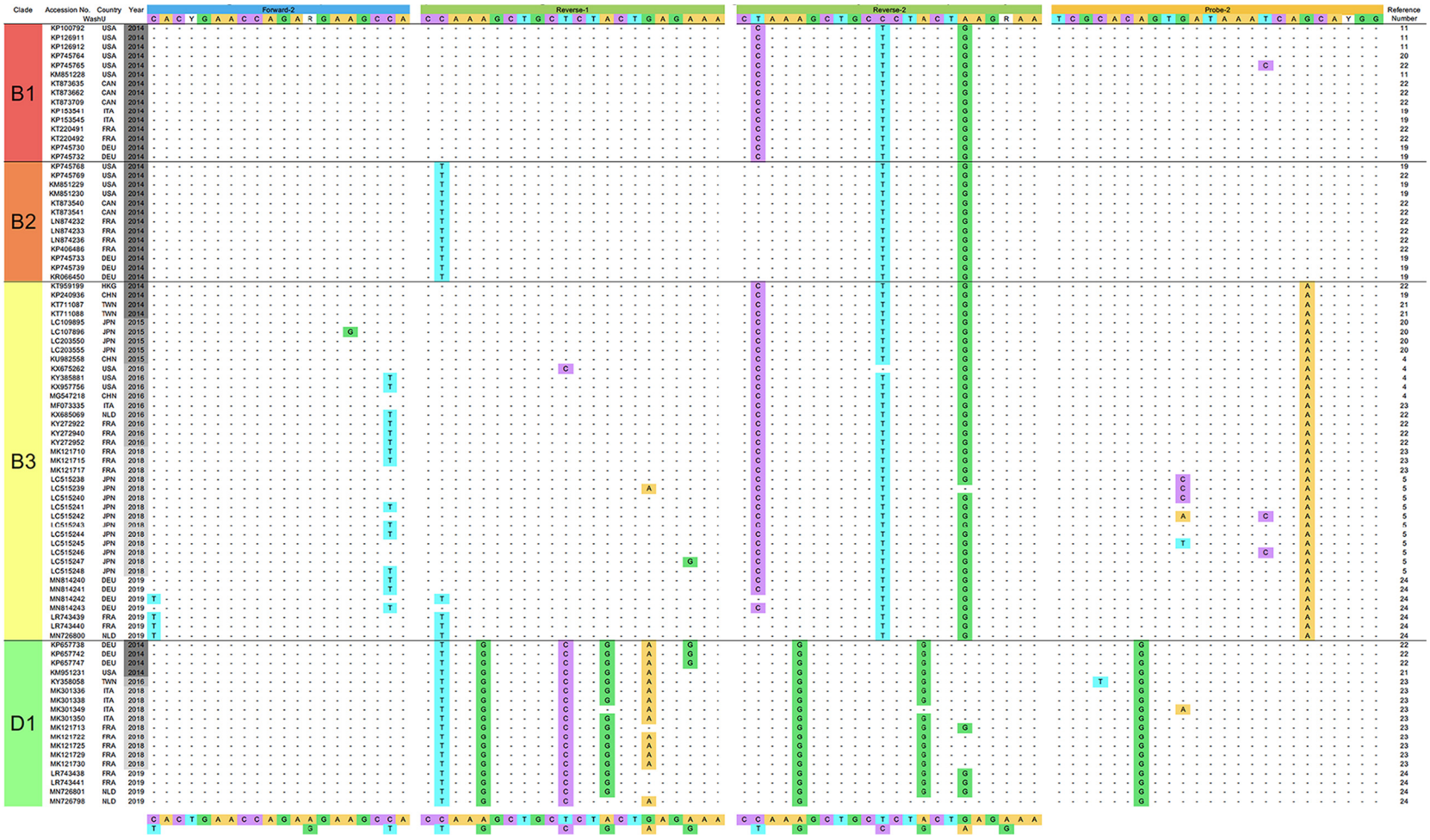

TABLE 2 Primers and probes used for PCR amplification and sequencing of enterovirus D68[a]

Method	Name	Primer or probe	Sequence (5′–3′)	Sense or antisense	Gene	Position[b]	Concn (μM)	Thermal conditions (amplicon size)
Real-time PCR	NU assay	Forward	ACTGAACCAGARGAAGCYA	Sense	VP1	2498–2516	0.6	42°C for 5 min, followed by 95°C for 10 s, and 40 cycles of 95°C for 15 s and 55°C for 45 s (~94 bp)
		Reverse	AAAGCTGCTCTACTGAGAA	Antisense	VP1	2574–2592	0.4	
		Reverse-2	AAGGCTGCCCTGCTRAGAA	Antisense	VP1	2574–2592	0.4	
		Probe	TCGCACAGTNATAAAYCARCAYGG	Sense	VP1	2524–2547	0.3	
Seminested/ nonnested PCR	CDC 1	AN1019	GCIATGYTNGGNACNCA	Sense	VP3	2088–2103	1.0	95°C for 3 min, followed by 40 cycles at 95°C for 30 s, 42°C for 30 s (0.4°C/s), and 60°C for 90 s (~1,380 bp)
		AN1014	CARTARTAAACICCNGTRTTRCA	Antisense	2A	3443–3465	1.0	
	CDC 4	AN1021	GCAGCAAARGAYGAYTT	Sense	VP3	2297–2313	0.8	95°C for 3 min, followed by 40 cycles at 95°C for 30 s, 52°C for 20 s, and 72°C for 60 s (~590 bp)
		AN1022	TTACTGCCKGAYTGCCARTGRAA	Antisense	VP1	2870–2892	0.8	
	N-Set	N-1	AATGCAGTTGAAACAGGTGC	Sense	VP1	2468–2487	0.8	95°C for 3 min, followed by 40 cycles at 95°C for 30 s, 60°C for 20 s, and 72°C for 15 s (~390 bp)
		N-2	ACCAGTRGGTACAAACATTGC	Antisense	VP1	2822–2842	0.8	

[a]Abbreviations: NU, Niigata University; CDC, Centers for Disease Control and Prevention.
[b]The positions of all primers and probes are given relative to the genome of enterovirus D68 (GenBank accession number MN726800).

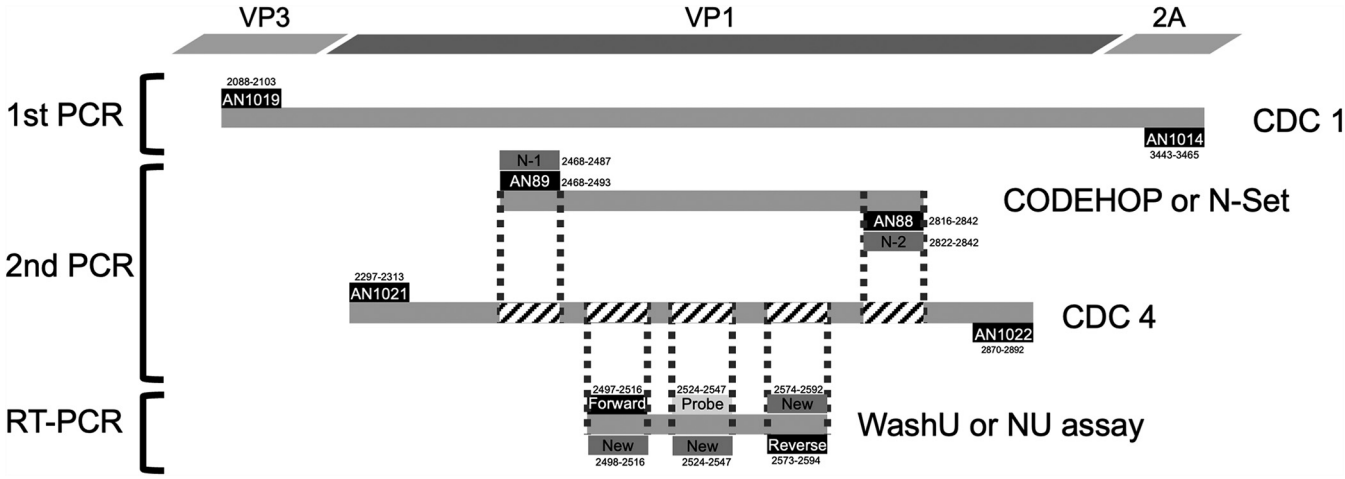

FIG 1 Position of each primers and probes for real-time PCR and seminested PCR. Primers and probes for real-time PCR and seminested PCR are located in the viral protein 1 region of enterovirus D68 (EV-D68). The targeting regions of the seminested PCR assays contain the targeting regions of the EV-D68-specific real-time PCR assays.

variants (referred to here as the Niigata methods): EV-D68-specific real-time PCR and nonnested PCR (Table 2).

New EV-D68-specific real-time PCR (Niigata University assay). Real-time PCR was performed using the One-Step PrimeScript RT-PCR kit (TaKaRa, Tokyo, Japan) and the Thermal Cycler Dice Real Time System III (TaKaRa). The 20-μl PCR mixture contained 2 μl of extracted RNA, 0.6 μM forward primer, 0.4 μM reverse primer, 0.3 μM TaqMan probe, 10 μl of 2 $\times$ One Step RT-PCR buffer III, 0.4 μl of TaKaRa *Ex Taq* HS (5 U/μl), and 0.4 μl of PrimeScript RT enzyme Mix II. The thermal cycling conditions were 42°C for 5 min, followed by 95°C for 10 s and then 45 cycles of 95°C for 15 s and 55°C for 45 s. The thermocycling settings were optimized based on the manufacturer's instructions for reagents and the thermal cycler used in this study. The reactions were run using Thermal Cycler Dice Real Time System III and analyzed using the accompanying threshold cycle (C_T) analysis software. To create the standard curve for the quantitation, we performed real-time PCR with serial dilution of designed double-stranded DNA (reference sequence LC515244) with different concentrations from 10^1 to 10^7 copies/μl. Each concentration of the samples was tested in triplicates, and the standard curve was made selecting the measurements closest to each concentration. The samples were tested simultaneously with the standard viral RNA (10^3 copies/μl) in triplicates in the assay, and the viral RNA level of the sample was quantified by the C_T values reflecting the standard value on the curve.

EV-D68-specific seminested PCR (CDC 1 and 4). After viral RNA was converted to cDNA with SuperScript VILO MasterMix (Invitrogen, Carlsbad, CA), nested PCR for the VP1 region was performed for EV-D68-positive samples using primers contributed by Allan Nix from the U.S. CDC (unpublished data) (Table 2) (5). For the first PCR, the 20-μl PCR mixture contained 2 μl of cDNA, 1.0 μM each primer (AN1019 and AN1014; CDC 1), and 10 μl of iQ Supermix (Bio-Rad Laboratories, Hercules, CA). The cycling conditions were 95°C for 3 min, followed by 40 cycles at 95°C for 30 s, 42°C for 30 s (0.4°C/s), and 60°C for 90 s. For the second PCR, the 20-μl PCR mixture contained 2 μl of the first PCR product, 0.8 μM concentrations of each primer (AN1021 and AN1022; CDC 4), and 10 μl of iQ Supermix. The cycling conditions were 95°C for 3 min, followed by 40 cycles at 95°C for 30 s, 52°C for 20 s, and 72°C for 60 s. The PCR products were purified by using the ExoSAP-IT Express (Thermo Fisher Scientific, Waltham, MA) and sequenced with a BigDye Terminator v3.1 cycle sequencing kit (Applied Biosystems, Foster City, CA) on an automated sequencer (Applied Biosystems 3130xl genetic analyzer).The samples were analyzed by sequencing and genotyping using BLAST analysis (https://blast.ncbi.nlm.nih.gov/Blast.cgi).

Modified seminested PCR assays (CDC 1 and Niigata University set). The primer binding regions of the second PCR of the CODEHOP approach were contained in the VP1 region sequenced by CDC 4 (Fig. 1). Using the strains detected in 2018 in Niigata and other past reports as reference, we identified the genetic variants of each region. To reflect genetic changes, we redesigned each primer of AN89 and AN88 for N-1 and N-2 (Niigata University set [N-Set]). After the first PCR (CDC 1), we performed the second PCR with NU Set (Table 2). For the second PCR, the 20-μl PCR mixture contained 2 μl of the first PCR product (CDC 1) and 0.8 μM concentrations of each primer (N-Set: N-1 and N-2). The cycling conditions were 95°C for 3 min, followed by 40 cycles at 95°C for 30 s, 60°C for 20 s, and 72°C for 15 s.

Nonnested PCR assays only with CDC 4 or N-Set. Nonnested PCR with the primer set of CDC 4 (AN1021 and AN1022) or N-Set (N-1 and N-2) was performed. After viral RNA was converted to cDNA, the 20-μl PCR mixture contained 2 μl of cDNA and each primer. The cycling conditions were same as described above.

Comparisons of assays. To compare assays, all assays were performed by using 22 EV-D68-positive samples. For real-time PCR, we compared positive rates and C_T values obtained by WashU (10) and the novel real-time PCR assay (NU assay). To compare the positive rates of two assays using the samples and

TABLE 3 Real-time PCR assay results for enterovirus, enterovirus/rhinovirus, WashU, and the Niigata University method for 22 EV-D68 samples[a]

Sample no.	C_T value				Viral RNA levels (log_{10} copies/μl)	ΔC_T[b]	Accession no.
	EV (17)	EV/rhino	WashU (10)	NU assay			
4	29.69	Negative	Negative*	25.17	3.93		LC515238
5	30.86	32.73	Negative*	26.37	3.57		LC515239
6	32.34	30.23	31.65	22.75	4.64	−8.9	LC627042
7	Negative	29.24	Negative*	34.38	1.20		LC627043
11	37.89	34.86	Negative*	31.31	2.11		LC627044
12	33.8	41.48	Negative*	33.28	1.52		LC627045
15	30.15	24.49	Negative*	36.09	0.69		LC627046
16	23.66	21.36	Negative*	18.06	6.04		LC515240
19	32.39	25.76	32.04	23.08	4.55	−8.96	LC515241
20	Negative	26.22	Negative*	30.29	2.41		LC515242
21	Negative	Negative	Negative*	35.19	0.96		LC627047
23	32.95	34.34	37.35	27.55	3.22	−9.8	LC515243
25	33.45	34.23	37.81	28.74	2.87	−9.07	LC515244
31	35.95	34.31	Negative*	30.04	2.48		LC515245
32	28.97	25.4	30.33	21.5	5.02	−8.83	LC627048
33	27.59	24.47	27.78	20.5	5.32	−7.28	LC627049
34	31.13	28.86	Negative*	26.28	3.60		LC515246
37	28.39	31.42	Negative*	26.12	3.65		LC627050
39	34.76	34.81	33.47	31.63	2.01	−1.84	LC627051
40	33.95	32.29	31.55	27.97	3.10	−3.58	LC515247
41	35.5	32.72	36.5	26.51	3.53	−9.99	LC515248
46	Negative	37.45	36.61	34.51	1.16	−2.1	LC627052
Positive rate[c]	82 (18/22)	91 (20/22)	45 (10/22)	100 (22/22)	3.16	−8.865	

[a]An asterisk (*) indicates a designated band was positive on electrophoresis. Abbreviations: EV, enterovirus; C_T, threshold cycles; EV/Rhino, enterovirus/rhinovirus; EP, electrophoresis; WashU, Washington University; NU, Niigata University.
[b]Calculated as follows: ΔC_T = NU assay – WashU assay.
[c]Calculated as follows: positive rates/median viral RNA level/median ΔC_T. The values in this row are expressed as "% (no. positive/no. tested)."

paired C_T values, we used the McNemar test and Wilcoxon signed-rank test for each and STATA software version 16.1 (Stata Corp., College Station, TX). In addition, we used the McNemar test to compare positive rates for the seminested PCR with CDC 1 and 4 (CDC 1/4) and nonnested PCR with N-Set. A two-sided P value of $<$5% was considered to indicate statistical significance.

Analysis of limit of detection of NU assay. The analytic limit of detection (LOD) for the NU assay was determined by testing up to 10 replicates of each concentration (0.5, 1, 5, and 10 copies/reaction.) of the EV-D68 DNA fragment (reference sequence LC515244) on two separate days. The proportion of the positive results obtained from each concentration was analyzed using probit regression analysis, which was carried out using R statistical software (version 4.1.0; R Foundation, Vienna, Austria). The theoretical LOD was based on the computer modeling approach and was defined as the exact theoretical copy number that would give a positive PCR response with a 95% probability.

Analyses of limit of detection of CDC4/N-Set and N-Set. The analytic LOD for these assays were determined by testing up to 10 replicates of concentrations (0.5, 1, 5, and 10 copies/reaction) of converted cDNA of EV-D68 (LC515238). Each theoretical LOD was calculated by probit regression analysis as performed for the NU assay.

Viral genome sequences for *in silico* sensitivity and specificity analyses. We obtained the virus genome sequences belonging to *Picornaviridae*, EV, and EV-D68 lineages from the National Center for Biotechnology Information (NCBI) virus database (25). For further analysis, we created a non-EV-D68 EV genome set (EV genomes minus EV-D68 genomes) and a non-EV-D68 *Picornaviridae* genome set (*Picornaviridae* genomes minus EV genomes). In total, we used 540 EV-D68 genome sequences, 3,683 non-EV-D68 EV genome sequences, and 1,721 non-EV *Picornaviridae* genome sequences. There were four clades of EV-D68 due to the diversity of VP1 gene sequences (20). To validate each clade, the VP1 sequence for each clade was obtained from GenBank (26) based on the clade classification performed previously (25).

***In silico* sensitivity and specificity analysis for each primer and probe to virus sequences.** To calculate the complementarity of each primer and probe, we aligned them using BLAST (27) with the blastn-short option. Using the results of the complementarity, we counted the numbers of mismatches of each primer and probe and organized the results by each clade (A, B1, B2, B3, C, and D) and period (1962 to 2013 and 2014 to 2018) for the *in silico* sensitivity analyses. To compare the sensitivity of the WashU assay, we performed the same analyses for the WashU assay. For the specificity analyses, the percentage of matched residues for primer sequence length was defined as an identity, and the criterion for the presence or absence of complementarity was whether the identity was equal to or greater than

TABLE 4 Seminested/nonnested PCR assay results for enterovirus, enterovirus/rhinovirus, WashU, and Niigata University methods for 22 EV-D68 samples[a]

Sample no.	CODEHOP (16)	CDC 1/4	CDC 1/N-Set	CDC 4/N-Set	Nonnested PCR (CDC 4)	Nonnested PCR (N-Set)	Viral RNA level (log_{10} copies/μl)[b]	Accession no.
4	Negative	Positive	Positive	Positive	Negative	Positive	3.93	LC515238
5	Negative	Positive	Positive	Positive	Negative	Positive	3.57	LC515239
6	Negative	Negative	Positive	Multiband	Positive	Positive	4.64	LC627042
7	Negative	Negative	Negative	Positive	Negative	Positive	1.20	LC627043
11	Negative	Negative	Negative	Negative	Negative	Positive	2.11	LC627044
12	Negative	Negative	Positive	Multiband	Negative	Positive	1.52	LC627045
15	Negative	Negative	Negative	Negative	Negative	Positive	0.69	LC627046
16	Positive	Positive	Positive	Multiband	Positive	Positive	6.04	LC515240
19	Negative	Positive	Positive	Multiband	Positive	Positive	4.55	LC515241
20	Negative	Positive	Negative	Positive	Negative	Positive	2.41	LC515242
21	Negative	Negative	Negative	Positive	Negative	Negative	0.96	LC627047
23	Negative	Positive	Positive	Multiband	Positive	Positive	3.22	LC515243
25	Negative	Positive	Positive	Multiband	Positive	Positive	2.87	LC515244
31	Negative	Positive	Positive	Multiband	Positive	Positive	2.48	LC515245
32	Negative	Negative	Positive	Multiband	Positive	Positive	5.02	LC627048
33	Positive	Negative	Positive	Multiband	Negative	Positive	5.32	LC627049
34	Negative	Positive	Positive	Negative	Negative	Positive	3.60	LC515246
37	Positive	Negative	Positive	Multiband	Negative	Positive	3.65	LC627050
39	Negative	Negative	Positive	Positive	Negative	Positive	2.01	LC627051
40	Negative	Positive	Positive	Multiband	Negative	Positive	3.10	LC515247
41	Negative	Positive	Positive	Multiband	Negative	Positive	3.53	LC515248
46	Negative	Negative	Negative	Positive	Negative	Negative	1.16	LC627052
Positive rate[c]	14 (3/22)	50 (11/22)	73 (16/22)	32 (7/22)	32 (7/22)	91 (20/22)		

[a]Abbreviations: CODEHOP, consensus degenerate hybrid oligonucleotide primer approach; CDC, Centers for Disease Control and Prevention; N, Niigata.
[b]Viral RNA levels were calculated as cycle threshold values of our novel enterovirus D68 real-time PCR assay.
[c]Calculated as follows: positive rates/median viral RNA level/median ΔC_T. The values in this row are expressed as "% (no. positive/no. tested)."

80%. We verified whether the complementarity of each primer and probe for non-EV-D68 EV genome sequences and non-EV *Picornaviridae* genome sequences would be absent.

Approach for samples collected from AFP cases during EV-D68 outbreaks in Japan. To validate the two new assays, we used real-time PCR (NU assay) to analyze extracted RNA stored in our laboratory and collected samples from children with AFP during the EV-D68 outbreak in Japan (September through November in 2015 and 2018) (see Table S2B). If the NU assay was positive, we performed VP1 sequencing with the N-Set and CDC4/N-Set, using the same samples. In addition, WashU was also performed for all samples.

Phylogenetic analysis to determine EV-D68 clade. Using Molecular Evolutionary Genetics Analysis software, version 6 (MEGA6) (28), after multiple alignments with the ClustalW program, we identified the best substitution model, as indicated by the lowest Bayesian Information Criterion scores. A phylogenetic tree was constructed by using the maximum-likelihood method with Tamura three-parameter and discrete gamma distribution with five rate categories and 1,000 bootstrap replicates and partial VP1 region sequences for EV-D68 strains detected in reports published from 2014 through 2020 (4, 5, 13, 21, 23, 24).

RESULTS

Evaluation of novel EV-D68-specific real-time PCR (NU assay). The standard curve for the novel real-time PCR assay is shown in Fig. S1. To evaluate the sensitivity and specificity of the novel assays, we tested 22 EV-D68 samples and 135 non-EV-D68 samples, respectively.

We confirmed that all 22 EV-D68 samples (100%) were positive with the novel EV-D68-specific real-time PCR (NU assay). To compare this assay to the previously reported assays, we assessed test positivity and C_T values for non-EV-D68-specific EV real-time PCR (17), non-EV-D68-specific EV/hRV real-time PCR (29), the WashU assay (10), and our novel real-time PCR using the same 22 EV-D68-positive nasopharyngeal samples simultaneously. Compared to the other assays, the novel real-time PCR assay yielded the highest positive rates (100% versus 45% for WashU; $P < 0.01$) and the lowest C_T values (median 27.76) (Tables 3 and 4). The median change in C_T value (NU assay − WashU assay) was −8.87 ($P = 0.005$). To evaluate specificity, we used the new real-time PCR to analyze 135 non-EV-D68 viral samples, including samples of EVs (94 samples), hRV (15

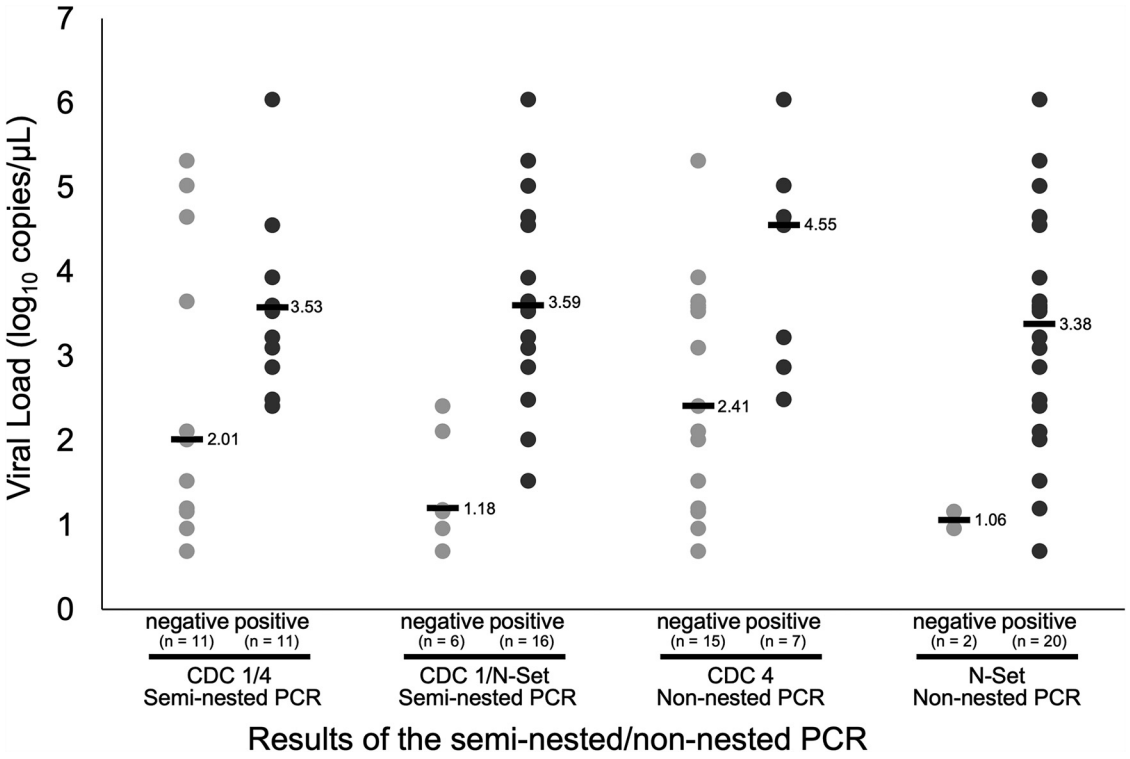

FIG 2 Comparison of each viral RNA level measured by the four PCR assays. We compared seminested PCR assay (CDC 1/4), seminested PCR (CDC 1/N-Set), nonnested PCR (CDC 4), and nonnested PCR (N-Set). The scatterplot shows the associations of viral RNA levels measured by the four assays. Each dot represents a viral RNA level. The bars represent median viral RNA levels.

samples), and non-EV/hRV (26 samples). All samples were negative with the novel assay (specificity, 100%).

EV-D68-specific seminested PCR for VP1 sequencing (CDC 1 and N-Set). The novel EV-D68-specific seminested PCR assay comprising CDC 1/N-Set was positive for 16/22 samples (73%) (Tables 3 and 4). The distribution of the viral RNA levels is shown in Fig. 2.

EV-D68-specific nonnested PCR for VP1 sequencing (CDC 4 or N-Set). EV-D68-specific nonnested PCR with CDC 4 or N-Set was positive for 7/22 samples (32%) and 20/22 samples (91%), respectively. The nonnested PCR with N-Set yielded a higher positive rate (91%, $P < 0.01$) than the CDC assays (CDC 1/4, 50%) (Tables 3 and 4). When CDC 1/4 were used, the samples with relatively high viral RNA levels ($>$3.50 log_{10} copies/μl) were negative; however, when N-Set were used, samples with high and relatively low RNA levels could be detected (Fig. 2). The lowest viral RNA level detected by the new assay was 0.69 log_{10} copies/μl.

Sensitivity analysis of novel EV-D68-specific real-time PCR (NU assay). The LOD of the NU assay was determined by the probit regression analysis (see Fig. S3). The probit regression analysis showed that a 95% LOD of the NU assay was 1.64 copies/reaction. The 95% LOD was corresponding to 492 copies/ml in nasopharyngeal, oropharyngeal, serum, and CSF samples for the extraction kit (QIAamp MinElute Virus Spin kit [Qiagen, Valencia, CA]) used in the present study.

Sensitivity analyses of novel EV-D68-specific seminested PCR (CDC4/N-Set) and nonnested PCR (N-Set). Each LOD of CDC4/N-Set and N-Set was determined by the probit regression analysis (see Fig. S4). The probit regression analysis showed that 95% LODs of CDC4/N-Set and N-Set were 1.16 and 1.92 copies/reaction, respectively.

***In silico* sensitivity and specificity analyses of the NU assay and N-Set.** In our *in silico* analyses, the current real-time PCR assay (NU assay) has a lower *in silico* sensitivity for clade A than the WashU assay; however, the NU assay showed higher *in silico*

TABLE 5 *In silico* analysis of each primer and probe in the NU and WashU assays for each clade[a]

	WashU					NU				
		No. of mismatches (%)					No. of mismatches (%)			
Clade (*n*)	Primer/probe (10)	0	1	2	≥3	Primer/probe	0	1	2	≥3
A (47)	L1-2	91.5	4.3	4.3	0.0	Forward	23.4	0.0	0.0	76.6
	R1-2	0.0	0.0	0.0	100.0	Reverse	0.0	0.0	0.0	100.0
	R2-2	0.0	78.7	14.9	6.4	Reverse-2	12.8	78.7	0.0	8.5
	P1-2	80.9	19.1	0.0	0.0	Probe	83.0	14.9	0.0	2.1
B1 (221)	L1-2	93.2	5.9	0.5	0.5	Forward	93.2	5.9	0.0	0.9
	R1-2	94.1	4.5	0.5	0.9	Reverse	94.1	1.4	0.0	4.5
	R2-2	0.0	0.0	0.5	99.5	Reverse-2	0.0	0.5	2.7	96.8
	P1-2	95.5	3.2	1.4	0.0	Probe	98.6	0.5	0.0	0.9
B2 (13)	L1-2	100.0	0.0	0.0	0.0	Forward	84.6	0.0	0.0	15.4
	R1-2	0.0	7.7	84.6	7.7	Reverse	76.9	7.7	0.0	15.4
	R2-2	0.0	0.0	92.3	7.7	Reverse-2	0.0	0.0	0.0	100.0
	P1-2	92.3	7.7	0.0	0.0	Probe	84.6	0.0	0.0	15.4
B3 (165)	L1-2	30.3	1.2	64.2	4.2	Forward	95.2	2.4	0.6	1.8
	R1-2	95.2	2.4	0.0	2.4	Reverse	94.5	2.4	0.0	3.0
	R2-2	0.0	0.0	0.6	99.4	Reverse-2	0.0	0.0	0.0	100.0
	P1-2	0.0	88.5	0.6	1.8	Probe	94.5	2.4	0.6	2.4
C (59)	L1-2	89.8	8.5	1.7	0.0	Forward	100.0	0.0	0.0	0.0
	R1-2	0.0	0.0	1.7	98.3	Reverse	1.7	30.5	64.4	3.4
	R2-2	0.0	30.5	69.5	0.0	Reverse-2	0.0	0.0	0.0	100.0
	P1-2	98.3	1.7	0.0	0.0	Probe	100.0	0.0	0.0	0.0
D (28)	L1-2	100.0	0.0	0.0	0.0	Forward	96.4	0.0	0.0	3.6
	R1-2	0.0	0.0	0.0	100.0	Reverse	0.0	0.0	0.0	100.0
	R2-2	0.0	17.9	78.6	3.6	Reverse-2	67.9	7.1	3.6	21.4
	P1-2	3.6	85.7	0.0	10.7	Probe	3.6	82.1	0.0	14.3

[a]Abbreviations: WashU, Washington University; NU, Niigata University.

sensitivities for clades B3 and D due to decreased mismatch for primers and probe (Table 5). Moreover, we calculated the mismatch numbers for each primer and probe for old strains (1962 to 2013) and recent strains (2014 to 2018). The WashU assay showed increasing mismatches for the forward primer (L1-2) and the probe (P1-2) and decreasing them for one of the reverse primers (R1-2). In contrast, the NU assay showed relatively lower *in silico* sensitivities for old strains; however, the NU assay showed higher sensitivities for each primer and probe for recent strains (Table 6). Regarding N-Set, N-1 and N-2 have high sensitivities for recent strains (see Table S8). For the *in silico* specificity analysis, no genome sequence with an identity >80% was found in non-EV-D68 *Picornaviridae* sequences except for N-2 (see Table S9). Thus, we

TABLE 6 *In silico* analysis of each assay for two periods (1962 to 2013 and 2014 to 2018)[a]

	WashU				NU			
		No. of mismatches (%)				No. of mismatches (%)		
Period (*n*)	Primer/probe (10)	0	1	≥2	Primer/probe	0	1	≥2
1962-2013 (136)	L1-2	83.1	5.1	11.8	Forward	62.5	4.4	33.1
	R1-2	16.9	2.2	80.9	Reverse	7.4	14.0	78.7
	R2-2	0.0	44.1	59.6	Reverse-2	4.4	31.6	64.7
	P1-2	73.5	11.8	14.7	Probe	83.1	6.6	9.6
2014-2018 (396)	L1-2	66.4	2.8	30.8	Forward	94.7	2.8	2.5
	R1-2	86.1	3.0	10.9	Reverse	87.9	1.5	10.4
	R2-2	0.0	0.0	100.0	Reverse-2	5.6	0.5	94.2
	P1-2	50.8	40.2	9.1	Probe	90.7	6.1	3.3

[a]Abbreviations: WashU, Washington University; NU, Niigata University.

TABLE 7 EV-D68 detection in patients with acute flaccid myelitis[a]

Sample no.	Yr	Diagnosis	Sample type	Assay result (C_T)		Accession no.
				NU	WashU	
1	2015	AFM	Serum	Negative	Negative	LC627053
			CSF	Negative	Negative	LC627053
			OP	Positive (21.8)	Positive	LC627053
			Stool	Positive (35.5)	Negative	LC627053
2	2018	AFM	Serum	Positive (38.7)	Negative	LC627054
			CSF	Negative	Negative	LC627054
			OP	Positive (33.3)	Negative	LC627054
3	2018	AFM	Serum	Negative	Negative	LC627055
			CSF	Negative	Negative	LC627055
			OP	Positive (36.5)	Negative	LC627055

[a]Abbreviations: NU, Niigata University; AFM, acute flaccid myelitis; CSF, cerebrospinal fluid; OP, oropharyngeal; C_T, threshold cycle value. Sequence analysis for viral protein 1 was performed with the N-Set or CDC4/N-Set. All samples were found to belong to the clade B3 branch by sequence and phylogenetic analysis.

estimated that the NU assay did not show the cross-reactivity for non-EV-D68 viruses.

Detection of EV-D68 in samples from AFM patients. We used the new real-time PCR (NU assay) to analyze 32 samples from 11 patients with AFP in 2015 or 2018, when EV-D68 outbreaks occurred in Japan. Five samples from three AFM patients (one in 2015 and two in 2018) were positive with the new assay, whereas only one sample was positive with the WashU assay (Table 7). Oropharyngeal samples were positive for all three positive cases, and EV-D68 clade B3 was identified in these three cases by sequence and phylogenetic analysis (see Fig. S4). These results show that the new real-time PCR assay successfully detected additional AFM EV-D68 cases that were not detected by the WashU assay. A total of 22 samples, including serum (n = 7), cerebrospinal fluid (n = 4), oropharyngeal (n = 7), and stool (n = 4) samples collected from 8 patients (72.7%), were determined to be negative by the NU and WashU assays.

Phylogenetic analysis to determine EV-D68 clade. Figure S5 shows the phylogenetic tree, including 11 newly detected samples collected in 2018 from patients with asthma-like respiratory illness, 3 samples from AFM patients, and other strains identified in the United States, Europe, China, and Japan. All samples collected in Niigata belonged to the clade B3 branch.

DISCUSSION

The present findings demonstrate the value of our novel EV-D68-specific real-time (NU assay) and nonnested PCR assays (N-Set). Compared to assays commonly used worldwide since 2014, these new assays had higher sensitivity, which could lead to more accurate diagnosis of recent strains of EV-D68. In addition, our new nonnested PCR assay was able to sequence the VP1 region with higher sensitivity, which improved clade identification of recent EV-D68 strains.

EV-D68 infection is associated with upper and lower respiratory disease and AFM (21). EV-D68 has caused worldwide biennial outbreaks since 2014 and is likely to continue to circulate around the world (5). In the United States and Europe, EV-D68 national surveillance for respiratory infections is ongoing, and EV-D68 was detected by direct EV-D68-specific real-time PCR or EV-D68-specific real-time PCR after a positive EV or EV/hRV real-time PCR result (6, 7). In addition, cases of EV-D68-related AFM have been collected in AFP global surveillance. Although EV-D68 is the predominant pathogen in AFM (30), the detection rate of EV-D68 in biological specimens from AFM patients has been limited (range, 6 to 60%) (31). The site-specific immunological response to EV-D68 may lead to negative PCR results in certain biological samples, which could potentially miss EV-D68 diagnosis in AFM patients (31, 32). Therefore, both epidemiological and biological evidence of EV-D68 is necessary in order to show an association between EV-D68 and AFM (30). To clarify the linkage between the epidemiological evidence of EV-D68 and AFM, surveillance of EV-D68 respiratory disease is essential because EV-D68 mainly causes

respiratory illnesses (33). In AFM cases, EV-D68 was detected from respiratory sample most frequently (34); however, in our study, seven throat samples of eight AFP patients were negative for EV-D68-specific real-time PCR. The possible reasons include the patients had infection other than EV-D68 infection or had a site-specific immunological response to EV-D68 without active viral infection.

Direct EV-D68 detection with EV-D68-specific real-time PCR has become a standard technique because of its convenience, speed, and precision. The WashU assay has been widely used to detect EV-D68 infection and is more sensitive than the CDC assay (10). However, the probe for the WashU assay did not bind to more recent EV-D68 strains containing variant sequence in the VP1 region (5). Our sequence analyses revealed that a part of EV-D68 detected after 2014 exhibited genetic changes in the primer and probe binding sites (Table 1; see also Tables S3 to S5). Regarding seminested PCR for EV-D68 VP1 sequencing, traditional assays, such as those using the CODEHOP approach, have become unsatisfactory because of recent genetic changes (Table 1; see also Tables S3 to S5). Therefore, sequences around each primer and probe binding site must be monitored, and assays accordingly revised, to ensure detection of EV-D68 with genetic changes.

The reverse primer of the novel real-time PCR assay was optimized for all recent clades except clade D1 (Table 1). The WashU assay has two reverse primers: one is optimized for strains circulating in 2014 (R2-1), the other was designed for future variants (R2-2) (10). Consequently, R2-2 tended to be suitable for clade D1 (Table 1). To optimize for the recent clade D1, we redesigned R2-2 as "Reverse-2" (Table 2; see also Fig. S2) to detect clade D1 more specifically.

In addition to EV-D68, influenza virus and severe acute respiratory syndrome coronavirus 2 (SARS-CoV-2) have undergone genetic mutations and require multiple assays to ensure accurate diagnosis (35, 36). The evolution of SARS-CoV-2, and the resulting genetic changes to assay binding sites, has decreased the sensitivity of SARS-CoV-2 real-time PCR assays (37). Similarly, because EV-D68 has evolved since 2014, diagnostic assays must be monitored and adapted. Our nonnested PCR assay (N-Set) includes the region targeted by the real-time PCR assay (Fig. 1). Therefore, the nonnested PCR assay was able to monitor genetic changes in the real-time PCR targeting region. Compared to novel real-time PCR, the primer binding sites of N-Set (N-1 and N-2) have been highly conserved since 2014 (Table 1; see also Tables S3 to S5). Monitoring of genetic changes in the real-time PCR targeting region allows for easy updates of the real-time PCR assay when genetic variants are found.

In addition to the novel real-time PCR assay to detect EV-D68, the nonnested PCR assay using N-Set allows for phylogenetic analysis in EV-D68 surveillance. Since 2014, phylogenetic analysis has been used to determine EV-D68 clade (4, 5, 13, 14, 20, 23). Clade B3 has been the dominant clade, and clade D1 emerged as a causative pathogen in the 2018 European outbreaks (5). The relation of clade to clinical characteristics is not well understood and must be further investigated. N-Set can determine clade by phylogenetic analysis. After noting the decreased sensitivity of both WashU and CDC assay, we were initially concerned that the samples were from patients infected by different clades; however, all positive samples belonged to clade B3 (see Fig. S5). It is important to note that, because clade B3 caused worldwide outbreaks in 2018, an EV-D68 diagnosis might be missed by current assays.

In the present study, the nonnested PCR assay (N-Set) yielded positive results for 20/22 (91%) samples. When we analyzed the two negative samples, the viral RNA level quantified by real-time PCR (Tables 3 and 4) was 0.96 to 1.16 $\log_{10}$ copies/μl, which was lower than for samples identified as positive by the seminested PCR with CDC 1/4 (1.51 to 6.04 $\log_{10}$ copies/μl). We also amplified using CDC 4 as the first PCR and N-Set as the second PCR for the two samples, which yielded positive results for two of two (100%) samples. All these samples were negative when the combination of CDC 1/N-Set was used (Table 4 and Fig. 2). The samples with higher viral RNA levels (e.g., samples 6, 16, and 19 in Table 4) was only amplified by CDC 4 or N-Set (Table 4). The

combination of CDC 4/N-Set yielded two bands around 590 and 390 bp on electrophoresis, because these two PCR products were amplified by both of these sets. Therefore, the sensitivity of the seminested PCR with CDC4/N-Set was lower (7/22; 32%) than nonnested PCR with N-Set (20/22; 91%). In addition, sensitivity was lower for single PCR with CDC 4 (7/22; 32%) than for N-Set. Therefore, the combined CDC 4/N-Set is not ideal for detecting EV-D68 but could be an alternative method for samples yielding negative results for N-Set.

As mentioned above, detection of EV-D68 from biological specimens collected from AFM patients is usually unsuccessful. In AFM surveillance, samples from different anatomical sites need to be collected to detect microorganisms (38). For additional validation of the novel PCR assays, we performed assays of AFP cases that were undiagnosed during the Japan EV-D68 outbreaks in 2015 and 2018. We successfully detected an additional two cases from oropharyngeal samples collected from three AFM patients (Table 7). Recent AFM cases related to EV-D68 may have been underdiagnosed by commonly used assays, and our new assays may be able to detect EV-D68 in AFM samples. We also performed phylogenetic analysis to confirm clade. In the phylogenetic tree (see Fig. S5), the sequences obtained from three AFM patients belonged to the clade B3 branch and included other EV-D68 samples collected from asthma-like respiratory illness in Japan in 2018.

This study has some limitations. First, the novel assays were evaluated by using a limited number of samples from one region of Japan. Validation of the utility of these novel assays will require analyses of more samples from different regions and countries. Second, the NU assay showed a lower *in silico* sensitivity for clade A than the WashU assay; however, clade A has not been detected in recent years, and the NU assay showed higher *in silico* sensitivities for the recent strains (Table 6). Therefore, a decreased sensitivity for a certain less endemic clade may be negligible. Finally, because the nonnested PCR with N-Set did not detect all EV-D68 cases, a novel assay with higher sensitivity, in response to new viral mutation, should be investigated in the future.

Because of genetic changes in viruses, the sensitivity of traditional PCR assays to detect and sequence EV-D68 has been decreasing. Our new assays are more sensitive and can detect EV-D68 in samples that yield negative results with current assays. To prepare for future EV-D68 outbreaks, EV-D68-specific assays must be continuously monitored and updated.

SUPPLEMENTAL MATERIAL

Supplemental material is available online only.

SUPPLEMENTAL FILE 1, PDF file, 0.8 MB.

ACKNOWLEDGMENTS

We thank Allan Nix at the U.S. Centers for Disease Control and Prevention for providing information on primers for detecting EV-D68. We acknowledge David Kipler for editing the manuscript.

Support was provided by a Grant-in-Aid for Scientific Research from Niigata University.

REFERENCES

1. Midgley CM, Watson JT, Nix WA, Curns AT, Rogers SL, Brown BA, Conover C, Dominguez SR, Feikin DR, Gray S, Hassan F, Hoferka S, Jackson MA, Johnson D, Leshem E, Miller L, Nichols JB, Nyquist AC, Obringer E, Patel A, Patel M, Rha B, Schneider E, Schuster JE, Selvarangan R, Seward JF, Turabelidze G, Oberste MS, Pallansch MA, Gerber SI, Group E-DW, EV-D68 Working Group. 2015. Severe respiratory illness associated with a nationwide outbreak of enterovirus D68 in the USA (2014): a descriptive epidemiological investigation. Lancet Respir Med 3:879–887. https://doi.org/10.1016/S2213-2600(15)00335-5.
2. Schieble JH, Fox VL, Lennette EH. 1967. A probable new human picornavirus associated with respiratory diseases. Am J Epidemiol 85:297–310. https://doi.org/10.1093/oxfordjournals.aje.a120693.
3. Holm-Hansen CC, Midgley SE, Fischer TK. 2016. Global emergence of enterovirus D68: a systematic review. Lancet Infect Dis 16:e64–e75. https://doi.org/10.1016/S1473-3099(15)00543-5.
4. Shen L, Gong C, Xiang Z, Zhang T, Li M, Li A, Luo M, Huang F. 2019. Upsurge of enterovirus D68 and circulation of the new subclade D3 and subclade B3 in Beijing, China, 2016. Sci Rep 9:6073. https://doi.org/10.1038/s41598-019-42651-7.
5. Ikuse T, Aizawa Y, Yamanaka T, Habuka R, Watanabe K, Otsuka T, Saitoh A. 2021. Outbreak of enterovirus D68 among children in Japan-worldwide circulation of enterovirus D68 clade B3 in 2018. Pediatr Infect Dis J 40:6–10. https://doi.org/10.1097/INF.0000000000002889.
6. Kujawski SA, Midgley CM, Rha B, Lively JY, Nix WA, Curns AT, Payne DC, Englund JA, Boom JA, Williams JV, Weinberg GA, Staat MA, Selvarangan R, Halasa NB, Klein EJ, Sahni LC, Michaels MG, Shelley L, McNeal M, Harrison CJ, Stewart LS, Lopez AS, Routh JA, Patel M, Oberste MS, Watson JT, Gerber SI. 2019. Enterovirus D68-associated acute respiratory illness: New Vaccine Surveillance Network, United States, July-October, 2017 and 2018. MMWR Morb Mortal Wkly Rep 68:277–280. https://doi.org/10.15585/mmwr.mm6812a1.

7. Poelman R, Schuffenecker I, Van Leer-Buter C, Josset L, Niesters HG, Lina B, Group E-EE-Ds. 2015. European surveillance for enterovirus D68 during the emerging North American outbreak in 2014. J Clin Virol 71:1–9. https://doi.org/10.1016/j.jcv.2015.07.296.
8. Harvala H, Broberg E, Benschop K, Berginc N, Ladhani S, Susi P, Christiansen C, McKenna J, Allen D, Makiello P, McAllister G, Carmen M, Zakikhany K, Dyrdak R, Nielsen X, Madsen T, Paul J, Moore C, von Eije K, Piralla A, Carlier M, Vanoverschelde L, Poelman R, Anton A, López-Labrador FX, Pellegrinelli L, Keeren K, Maier M, Cassidy H, Derdas S, Savolainen-Kopra C, Diedrich S, Nordbø S, Buesa J, Bailly JL, Baldanti F, MacAdam A, Mirand A, Dudman S, Schuffenecker I, Kadambari S, Neyts J, Griffiths MJ, Richter J, Margaretto C, Govind S, Morley U, Adams O, Krokstad S, Dean J, et al. 2018. Recommendations for enterovirus diagnostics and characterization within and beyond Europe. J Clin Virol 101:11–17. https://doi.org/10.1016/j.jcv.2018.01.008.
9. World Health Organization. 2015. Enterovirus surveillance guidelines: guidelines for enterovirus surveillance in support of the Polio Eradication Initiative (2015), p 1–46. World Health Organization, Geneva, Switzerland.
10. Wylie TN, Wylie KM, Buller RS, Cannella M, Storch GA. 2015. Development and evaluation of an enterovirus D68 real-time reverse transcriptase PCR assay. J Clin Microbiol 53:2641–2647. https://doi.org/10.1128/JCM.00923-15.
11. Greninger AL, Naccache SN, Messacar K, Clayton A, Yu G, Somasekar S, Federman S, Stryke D, Anderson C, Yagi S, Messenger S, Wadford D, Xia D, Watt JP, Van Haren K, Dominguez SR, Glaser C, Aldrovandi G, Chiu CY. 2015. A novel outbreak enterovirus D68 strain associated with acute flaccid myelitis cases in the USA (2012–14): a retrospective cohort study. Lancet Infect Dis 15:671–682. https://doi.org/10.1016/S1473-3099(15)70093-9.
12. Eshaghi A, Duvvuri VR, Isabel S, Banh P, Li A, Peci A, Patel SN, Gubbay JB. 2017. Global distribution and evolutionary history of enterovirus D68, with emphasis on the 2014 outbreak in Ontario, Canada. Front Microbiol 8:257. https://doi.org/10.3389/fmicb.2017.00257.
13. Bal A, Sabatier M, Wirth T, Coste-Burel M, Lazrek M, Stefic K, Brengel-Pesce K, Morfin F, Lina B, Schuffenecker I, Josset L. 2019. Emergence of enterovirus D68 clade D1, France, August to November 2018. Euro Surveill 24. https://doi.org/10.2807/1560-7917.ES.2019.24.3.1800699.
14. Piralla A, Principi N, Ruggiero L, Girello A, Giardina F, De Sando E, Caimmi S, Bianchini S, Marseglia GL, Lunghi G, Baldanti F, Esposito S. 2018. Enterovirus D68 (EV-D68) in pediatric patients with respiratory infection: the circulation of a new B3 clade in Italy. J Clin Virol 99–100:91–96. https://doi.org/10.1016/j.jcv.2018.01.005.
15. Piralla A, Girello A, Premoli M, Baldanti F. 2015. A new real-time reverse transcription-PCR assay for detection of human enterovirus 68 in respiratory samples. J Clin Microbiol 53:1725–1726. https://doi.org/10.1128/JCM.03691-14.
16. Nix WA, Oberste MS, Pallansch MA. 2006. Sensitive, seminested PCR amplification of VP1 sequences for direct identification of all enterovirus serotypes from original clinical specimens. J Clin Microbiol 44:2698–2704. https://doi.org/10.1128/JCM.00542-06.
17. Mohamed N, Elfaitouri A, Fohlman J, Friman G, Blomberg J. 2004. A sensitive and quantitative single-tube real-time reverse transcriptase-PCR for detection of enteroviral RNA. J Clin Virol 30:150–156. https://doi.org/10.1016/j.jcv.2003.08.016.
18. Aizawa Y, Watanabe K, Oishi T, Hirano H, Hasegawa I, Saitoh A. 2015. Role of maternal antibodies in infants with severe diseases related to human parechovirus type 3. Emerg Infect Dis 21:1966–1972. https://doi.org/10.3201/eid2111.150267.
19. Böttcher S, Prifert C, Weißbrich B, Adams O, Aldabbagh S, Eis-Hübinger AM, Diedrich S. 2016. Detection of enterovirus D68 in patients hospitalized in three tertiary university hospitals in Germany, 2013 to 2014. Euro Surveill 21. https://doi.org/10.2807/1560-7917.ES.2016.21.19.30227.
20. Kaida A, Iritani N, Yamamoto SP, Kanbayashi D, Hirai Y, Togawa M, Amo K, Kohdera U, Nishigaki T, Shiomi M, Asai S, Kageyama T, Kubo H. 2017. Distinct genetic clades of enterovirus D68 detected in 2010, 2013, and 2015 in Osaka City, Japan. PLoS One 12:e0184335. https://doi.org/10.1371/journal.pone.0184335.
21. Wang G, Zhuge J, Huang W, Nolan SM, Gilrane VL, Yin C, Dimitrova N, Fallon JT. 2017. Enterovirus D68 subclade B3 strain circulating and causing an outbreak in the United States in 2016. Sci Rep 7:1242. https://doi.org/10.1038/s41598-017-01349-4.
22. Kramer R, Sabatier M, Wirth T, Pichon M, Lina B, Schuffenecker I, Josset L. 2018. Molecular diversity and biennial circulation of enterovirus D68: a systematic screening study in Lyon, France, 2010 to 2016. Euro Surveill 23:1700711. https://doi.org/10.2807/1560-7917.ES.2018.23.37.1700711.
23. Pellegrinelli L, Giardina F, Lunghi G, Uceda Renteria SC, Greco L, Fratini A, Galli C, Piralla A, Binda S, Pariani E, Baldanti F. 2019. Emergence of divergent enterovirus (EV) D68 sub-clade D1 strains, northern Italy, September to October 2018. Euro Surveill 24. https://doi.org/10.2807/1560-7917.ES.2018.24.7.1900090.
24. Midgley SE, Benschop K, Dyrdak R, Mirand A, Bailly JL, Bierbaum S, Buderus S, Böttcher S, Eis-Hübinger AM, Hönemann M, Jensen VV, Hartling UB, Henquell C, Panning M, Thomsen MK, Hodcroft EB, Meijer A. 2020. Co-circulation of multiple enterovirus D68 subclades, including a novel B3 cluster, across Europe in a season of expected low prevalence, 2019/20. Euro Surveill 25. https://doi.org/10.2807/1560-7917.ES.2020.25.2.1900749.
25. Brister JR, Ako-Adjei D, Bao Y, Blinkova O. 2015. NCBI viral genomes resource. Nucleic Acids Res 43:D571–D577. https://doi.org/10.1093/nar/gku1207.
26. NCBI Resource Coordinators. 2018. Database resources of the National Center for Biotechnology Information. Nucleic Acids Res 46:D8–D13. https://doi.org/10.1093/nar/gkx1095.
27. Camacho C, Coulouris G, Avagyan V, Ma N, Papadopoulos J, Bealer K, Madden TL. 2009. BLAST+: architecture and applications. BMC Bioinformatics 10:421. https://doi.org/10.1186/1471-2105-10-421.
28. Tamura K, Stecher G, Peterson D, Filipski A, Kumar S. 2013. MEGA6: Molecular Evolutionary Genetics Analysis, version 6.0. Mol Biol Evol 30:2725–2729. https://doi.org/10.1093/molbev/mst197.
29. Tapparel C, Cordey S, Van Belle S, Turin L, Lee WM, Regamey N, Meylan P, Mühlemann K, Gobbini F, Kaiser L. 2009. New molecular detection tools adapted to emerging rhinoviruses and enteroviruses. J Clin Microbiol 47:1742–1749. https://doi.org/10.1128/JCM.02339-08.
30. Murphy OC, Messacar K, Benson L, Bove R, Carpenter JL, Crawford T, Dean J, DeBiasi R, Desai J, Elrick MJ, Farias-Moeller R, Gombolay GY, Greenberg B, Harmelink M, Hong S, Hopkins SE, Oleszek J, Otten C, Sadowsky CL, Schreiner TL, Thakur KT, Van Haren K, Carballo CM, Chong PF, Fall A, Gowda VK, Helfferich J, Kira R, Lim M, Lopez EL, Wells EM, Yeh EA, Pardo CA, group Aw. 2021. Acute flaccid myelitis: cause, diagnosis, and management. Lancet 397:334–346. https://doi.org/10.1016/S0140-6736(20)32723-9.
31. Helfferich J, Knoester M, Van Leer-Buter CC, Neuteboom RF, Meiners LC, Niesters HG, Brouwer OF. 2019. Acute flaccid myelitis and enterovirus D68: lessons from the past and present. Eur J Pediatr 178:1305–1315. https://doi.org/10.1007/s00431-019-03435-3.
32. Mishra N, Ng TFF, Marine RL, Jain K, Ng J, Thakkar R, Caciula A, Price A, Garcia JA, Burns JC, Thakur KT, Hetzler KL, Routh JA, Konopka-Anstadt JL, Nix WA, Tokarz R, Briese T, Oberste MS, Lipkin WI. 2019. Antibodies to enteroviruses in cerebrospinal fluid of patients with acute flaccid myelitis. mBio 10:e01903-19. https://doi.org/10.1128/mBio.01903-19.
33. Itagaki T, Aoki Y, Matoba Y, Tanaka S, Ikeda T, Mizuta K, Matsuzaki Y. 2018. Clinical characteristics of children infected with enterovirus D68 in an outpatient clinic and the association with bronchial asthma. Infect Dis (Lond) 50:303–312. https://doi.org/10.1080/23744235.2017.1400176.
34. Ayers T, Lopez A, Lee A, Kambhampati A, Nix WA, Henderson E, Rogers S, Weldon WC, Oberste MS, Sejvar J, Hopkins SE, Pallansch MA, Routh JA, Patel M. 2019. Acute Flaccid Myelitis in the United States: 2015–2017. Pediatrics 144. https://doi.org/10.1542/peds.2019-1619.
35. World Health Organization. 2020. Laboratory testing for coronavirus disease 2019 (COVID-19) in suspected human cases: interim guidance, 2 March 2020, p 1–10. World Health Organization, Geneva, Switzerland.
36. World Health Organization. 2021. WHO information for molecular diagnosis of influenza virus: update, p 1–68. World Health Organization, Geneva, Switzerland.
37. Osório NS, Correia-Neves M. 2021. Implication of SARS-CoV-2 evolution in the sensitivity of RT-qPCR diagnostic assays. Lancet Infect Dis 21:166–167. https://doi.org/10.1016/S1473-3099(20)30435-7.
38. Messacar K, Asturias EJ, Hixon AM, Van Leer-Buter C, Niesters HGM, Tyler KL, Abzug MJ, Dominguez SR. 2018. Enterovirus D68 and acute flaccid myelitis-evaluating the evidence for causality. Lancet Infect Dis 18:e239–e247. https://doi.org/10.1016/S1473-3099(18)30094-X.